Monatshefte für Chemie 135, 1503–1517 (2004)
DOI 10.1007/s00706-004-0189-3

Monatshefte für Chemie
Chemical Monthly
Printed in Austria

Crystal Structure and Conformation of a Bilirubin Ester

Brahmananda Ghosh, Vincent J. Catalano, and **David A. Lightner***

Department of Chemistry, University of Nevada, Reno, Nevada 89557, USA

Received February 2, 2004; accepted February 11, 2004
Published online October 25, 2004

Summary. Crystal structures determined for three bilirubin analogs with *gem*-dimethyl groups at C(10) are reported, including the first X-ray structure of a bilirubin dimethyl ester. Conformation-determining torsion angles and key hydrogen bond distances and angles were compared to those from molecular dynamics calculations. Like other rubins, the component dipyrrinones of the three compounds were found to adopt the *syn* conformation, with *Z*-configuration double bonds at C(4) and C(15) and bis-lactam tautomeric structures of the end rings. No large differences in bond lengths and bond angles at C(10) were found, and the crystal structures of the two 10,10-dimethyl rubin acids showed considerable similarity to that of bilirubin: both pigments adopt a folded, intramolecularly hydrogen bonded ridge-tile conformation stabilized by six hydrogen bonds, with an interplanar angle in ridge-tile of ~98° and ~86°. In contrast, the dimethyl ester is intermolecularly hydrogen bonded in the crystal. Each molecule of the ester has its two *syn-Z*-dipyrrinones rotated into a conformation *syn* to the *gem*-dimethyl group, whereas in the acids they are *anti*.

Keywords. Bile pigments; Stereochemistry; Hydrogen bonding.

Introduction

Bilirubin is the yellow pigment of jaundice [1, 2] and is composed of two dipyrrinones conjoined to a CH_2 group [2, 3] (Fig. 1A). Its conformation is determined by relative orientation of the dipyrrinones about the C(10) CH_2 group, and while many conformations are possible, the most stable is shaped like a half-opened book, or a ridge-tile (Fig. 1B). The ridge-tile conformation minimizes intramolecular non-bonded steric interactions and is thus intrinsically favored over all others [4]. The conformation is further stabilized by a network of six intramolecular hydrogen bonds between the two dipyrrinones and the opposing propionic acids [4, 5]. Dipyrrinones are known to be avid participants in hydrogen bonding [3, 6], especially with carboxylic acids [7], even self-associating strongly to form hydrogen-bonded dimers [8]. The ridge-tile conformation is of course not rigid, and it is the

* Corresponding author. E-mail: lighter@scs.unr.edu

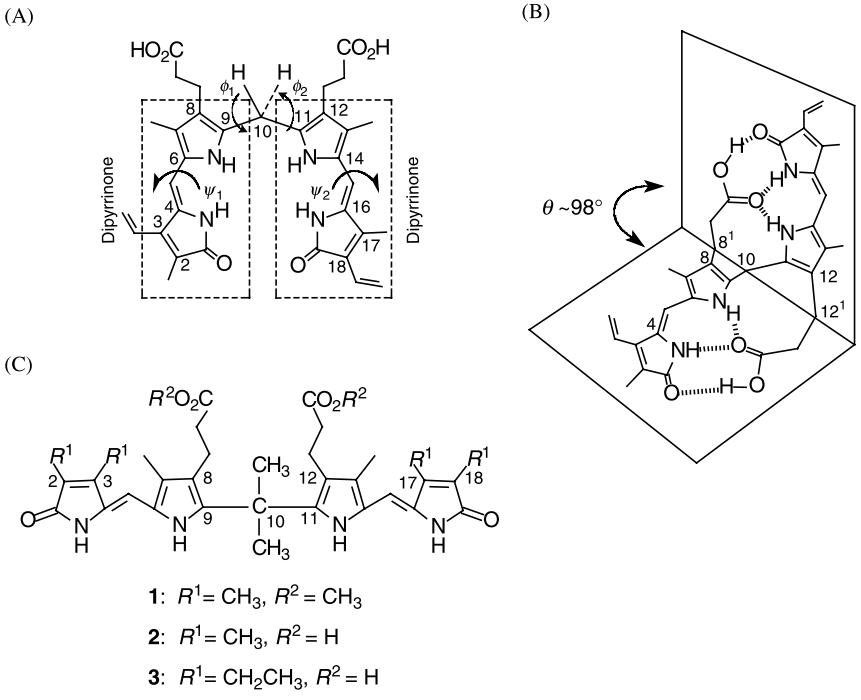

Fig. 1. Bilirubin, composed of two dipyrrinone chromophores, is shown in a porphyrin-like representation in (A) and in its ridge-tile-shaped energy minimum conformation in (B); conformation (B) achieves considerable stabilization from intramolecular hydrogen bonds (hatched lines); rotations about the C(9)–C(10) and C(10)–C(11) bonds, ϕ_1 and ϕ_2, converts bilirubin into a multitude of conformations; in (A) $\phi_1 = \phi_2 = 0°$, in (B) $\phi_1 = \phi_2 = 60°$; rotations about ψ_1 and ψ_2 within the two dipyrrinones distort the chromophores from planarity, in (B) the dipyrrinones are planar; in (C) the C(10) *gem*-dimethyl rubins **1**–**3** of this work are given

only conformation of bilirubin observed in crystals of bilirubin by X-ray crystallography [5, 9, 10] and by solid state NMR [11]. Solution NMR studies [12, 13] and circular dichroism spectroscopy [4, 14] confirm its dominance in solution, even when the carboxyl groups are ionized [13]. Molecular mechanics [3, 4, 15] and *Gaussian* 98 energy calculations [16] support the general belief that the ridge-tile conformation is very strongly stabilized.

Although a few crystal structures have been obtained for bilirubins [3, 5, 9, 10, 17, 18], none is apparently available for a diester (except for the bis-lactim methyl ether) [9]. The crystal structure of a 10-substituted bilirubin, 10-isopropyl-3,17-bis-normesobilirubin-XIIIα, showed that the presence of the isopropyl group caused the dihedral angle (θ of Fig. 1B) to open slightly while maintaining full intramolecular hydrogen bonding [17]. Earlier studies [19] showed that *gem*-dimethyl-rubins exhibited unusually enhanced solubility in polar solvents, suggesting that intramolecular hydrogen bonding was weakened by a *gem*-dimethyl effect. While the available NMR spectroscopic evidence indicated intramolecular hydrogen bonds between propionic acid and dipyrrinone groups [19b], in the absence of X-ray crystallographic data, it could not be ascertained clearly whether the hydrogen bonds were stretched or weakened by the presence of the *gem*-dimethyls at the "hinge" of the ridge-tile.

The preferred conformation of bilirubin dimethyl ester is less well understood. To the best of our knowledge there are no X-ray crystal structures available. ^{1}H NMR evidence suggests intermolecularly hydrogen-bonded structures in $CDCl_3$ with little or no hydrogen bonding between the propionic carbonyl groups and the dipyrrinones [12a, b]. In d_6-*DMSO*, the NMR evidence suggests a conformation similar to that of bilirubin with the CO_2CH_3 residues tied to the nearest pyrrole NH and lactam groups *via* bound solvent molecules [12c]. Vapor pressure osmometry (VPO) studies indicate dimer formation in nonpolar solvents such as CH_2Cl_2 [3, 20] – a general phenomenon for bilirubins without alkanoic acid groups at C(8)/C(12).

In the present communication, we describe X-ray crystal structures and molecular mechanics calculation investigations of 10,10-*gem*-dimethyl-rubin dimethyl ester **1** and acids **2** and **3** (Fig. 1C) – all of which are incapable of forming biliverdins. These results are compared to bilirubin X-ray crystal determinations and molecular dynamics calculations.

Results and Discussion

Configuration and Overall Conformation

An examination of the crystal structure drawing of the X-ray structure of dimethyl ester **1** shows that the CO_2CH_3 groups are *not* intramolecularly hydrogen bonded to the dipyrrinones (Fig. 2A). Rather, each dipyrrinone of one molecule is *inter*molecularly hydrogen bonded to a dipyrrinone of a neighboring molecule so as create supramolecular ribbons [21] or chains of linked tetrapyrroles (Fig. 2B). The shape of **1** is ridge-tile-like but extended, with the pyrrole nitrogens *syn* to the *gem*-dimethyls rather than *anti*, as found in **2** and **3**. This is a consequence of the dipyrrinones being rotated away from the porphyrin-like structure of Fig. 1A by $\phi_1 = 125°$, $\phi_2 = 133°$ (Table 1) – well past the ridge-tile (Fig. 1B), where $\phi_1 \sim \phi_2 \sim 60°$. Intermolecular hydrogen bonding has been detected in certain dipyrrinones in their X-ray crystal structures [3, 22], deduced from their ^{1}H NMR spectra in $CDCl_3$ by studying NH chemical shifts [6] and N*O*E experiments [13], and supported by vapor pressure osmometry (VPO) measurements that show dimers in solution in CH_2Cl_2 [23]. Bilirubin esters have also been studied by VPO [3, 20] and by ^{1}H NMR [12a, b], but the current work is the first crystal structure that clearly reveals a rubin ester conformation oriented in the crystal for dipyrrinone-to-dipyrrinone intermolecular hydrogen bonding.

In contrast, the crystal structure drawings of the X-ray structures of **2** and **3** clearly show structures with dipyrrinones in position for *intra*molecular hydrogen bonding to the opposing propionic acids (Figs. 3 and 4). The result is a ridge-tile conformation consistent with that found in crystals of bilirubin [5a, b, 10], mesobilirubin-IXα [5c], bilirubin bis-isopropyl ammonium salt [10], and 10-isopropylglaucorubin [17], with C(10) lying on the seam of the ridge-tile. The molecules pack in the crystal as stacked pairs of enantiomers (Fig. 4), similar to that seen in crystals of bilirubin [5a, b]. Solvent molecules (CH_2Cl_2 in **2**, $CHCl_3$ in **3**) are found in the crystals and take up positions so as to participate in hydrogen bonding. Curiously, given that **2** and **3** differ only in the methyl (**2**) *vs.* ethyl (**3**) lactam

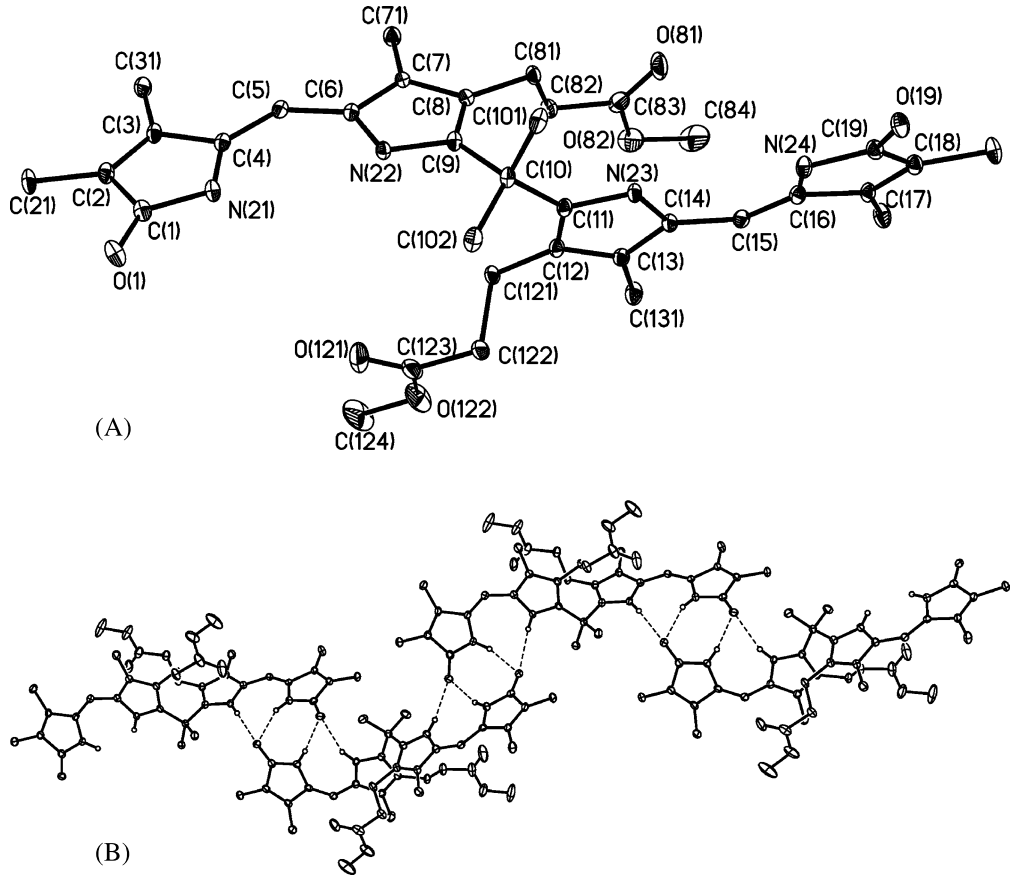

Fig. 2. (A) Crystal numbering system and crystal structure of ester **1** in a projection showing its extended conformation; (B) molecular packing of **1**, as observed in its crystal structure, with NH and OH hydrogens located and hydrogen bonds shown by dashed lines; librational ellipsoids have been drawn with 50% probability

substituents, the two planes containing the two dipyrrinones intersect at different interplanar angles (θ): 98° in **2** and 86° in **3**. The dihedral angle in **2** is the same as that found in bilirubin [5a, b] ($\theta \sim 98°$); whereas that in **3** is smaller – for reasons that are unclear but may involve crystal packing forces.

The apparent intramolecular hydrogen bond distances (Table 2) between the acids and dipyrrinones are ~0.2–0.3 Å longer in **2** and **3** than in bilirubin, indicating that the *gem*-dimethyls appear to cause the matrix of hydrogen bonds to stretch or weaken. This might explain the solubility of **2** and **3**, in polar solvents such as methanol, as compared to insoluble bilirubin. Yet, **2** and **3** are also more soluble than bilirubin in nonpolar solvents such as *n*-hexane or chloroform. The origin of the hydrogen bond stretching is not entirely clear because the conformation-determining torsion angles ϕ_1 and ϕ_2 are essentially the same as those of bilirubin (Table 1). The twist angles about the C(5)–C(6) and C(14)–C(15) single bonds ψ_1 and ψ_2 are smaller than in bilirubin, and the exocyclic double bonds are less twisted, which is consistent with flatter dipyrrinones in **2** and **3** than in bilirubin.

Table 1. Comparison of conformation determining torsion angles, (°) from X-ray crystallography and molecular dynamics (MD)[a] calculations for 10,10-dimethyl-rubins **1** and **2**, dimethyl ester **3**, and bilirubin (**BR**)

Structure/Method		ϕ_1 (11-10-9-22)[b]	ϕ_2 (9-10-11-23)[b]	ψ_1 (4-5-6-22)[c]	ψ_2 (16-15-14-23)[c]	(N21-4-5-6)[d]	(14-15-16-N24)[d]	θ (dipyrrinone)[e]	θ (pyrrole)[e]
1	X-ray	125	133	9.9	−4.3	3.8	4.7	(69)	(76)
	MD	54	52	11.5	2.6	0.6	0.5	102	103
2	X-ray	62	62	0.3	0.4	−6.2	0.5	98	102
	MD	60	60	9.5	9.6	0.0	0.0	93	93
3	X-ray	57	61	7.3	5.8	−2.6	3.2	86	87
	MD	60	60	−6.6	−7.5	−0.6	−0.6	92	91
BR[f]	X-ray	60	64	17.5	−2.7	10.7	5.8	98	99
	MD	59	58	16.1	16.1	1.0	−0.2	88	94

[a] Using Sybyl V. 6.9 for the SGI workstation, Refs. [4, 20]; [b] values are ∼0° for the porphyrin conformation, ∼60° for the ridge-tile conformation and, ∼180° for the linear conformation; [c] indicates distortion from a planar dipyrrinone, where $\psi \sim 0$; [d] indicates twist from 0° of C=C; [e] interplanar dihedral angle using the average plane of each dipyrrinone or the dihedral angle of the two pyrroles adjacent to C(10); [f] data taken from X-ray diffraction coordinates given in Ref. [5a]

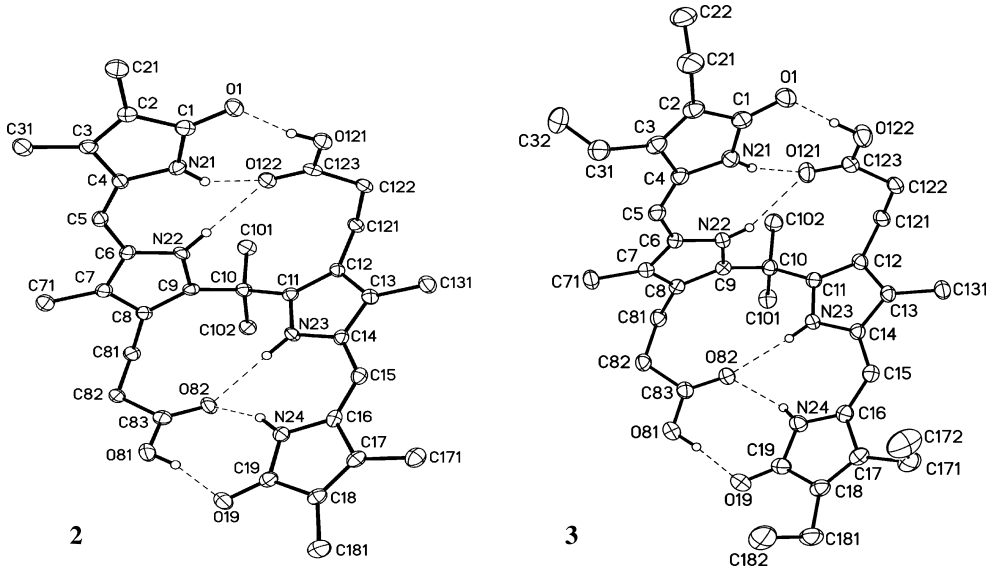

Fig. 3. Crystal numbering system and crystal structure drawing of **2** (left) and **3** (right), with NH and OH hydrogens located and hydrogen bonds shown by dashed lines; librational ellipsoids have been drawn with 50% probability

Flatter dipyrrinones imply longer hydrogen bonds and thus structures with an increased amphiphilicity relative to that of bilirubin. Except in these small details, the crystal structure ridge-tile conformations of **2** and **3** correlate reasonably well with that of bilirubin [5].

The dipyrrinones of **1**–**3** adopt a *syn-Z* configuration of the C=C at C(4) and C(15). The observed bond lengths suggest that delocalization over an individual conjugated system of two pyrrole rings is rather limited since C(4)=C(5) and C(15)=C(16) seem to be essentially full double bonds (average bond length of 1.35 Å). However, they are slightly longer than in bilirubin (average bond length of 1.30 Å). As suggested earlier for bilirubin [5a, b], mesobilirubin [5c], and its C(10)-isopropyl analog [17], *gem*-dimethyl-rubins **1**–**3** can be regarded as 2,2′-dipyrrylmethanes with conjugating substituents at the α positions.

It was shown previously that when the possibility of lactam/lactim tautomerism exists, the lactam form predominates [24] by about 4–10 orders of magnitude over the lactim form for bile pigments in solution [5c] and in all known rubin X-ray structures [5, 9, 10, 17, 18]. Thus it is not surprising that *gem*-dimethyl-rubins **1**–**3** adopt the bis-lactam tautomeric form, as confirmed by lactam C=O bond lengths that are comparable to C=O distances in ordinary lactams. In **1**, the C(1)=O(1) and C(19)=O(19) bond lengths are 1.24 Å, in **2** and **3** they are 1.25 Å, which compare favorably with those of 10-isopropylglaucorubin (1.25 Å) [17] and bilirubin [5a, b, 9] where the corresponding bond lengths are 1.25 and 1.28 Å, respectively. Furthermore, the lactam C–N bond distances are consistent with a carbon nitrogen *single* bond, C(1)–N(21) ~ C(19)–N(24) ~ 1.36 Å – again identical to those of 10-isopropylglaucorubin [17] and very similar to those found in bilirubin [5a–c] (1.41 and 1.35 Å, respectively).

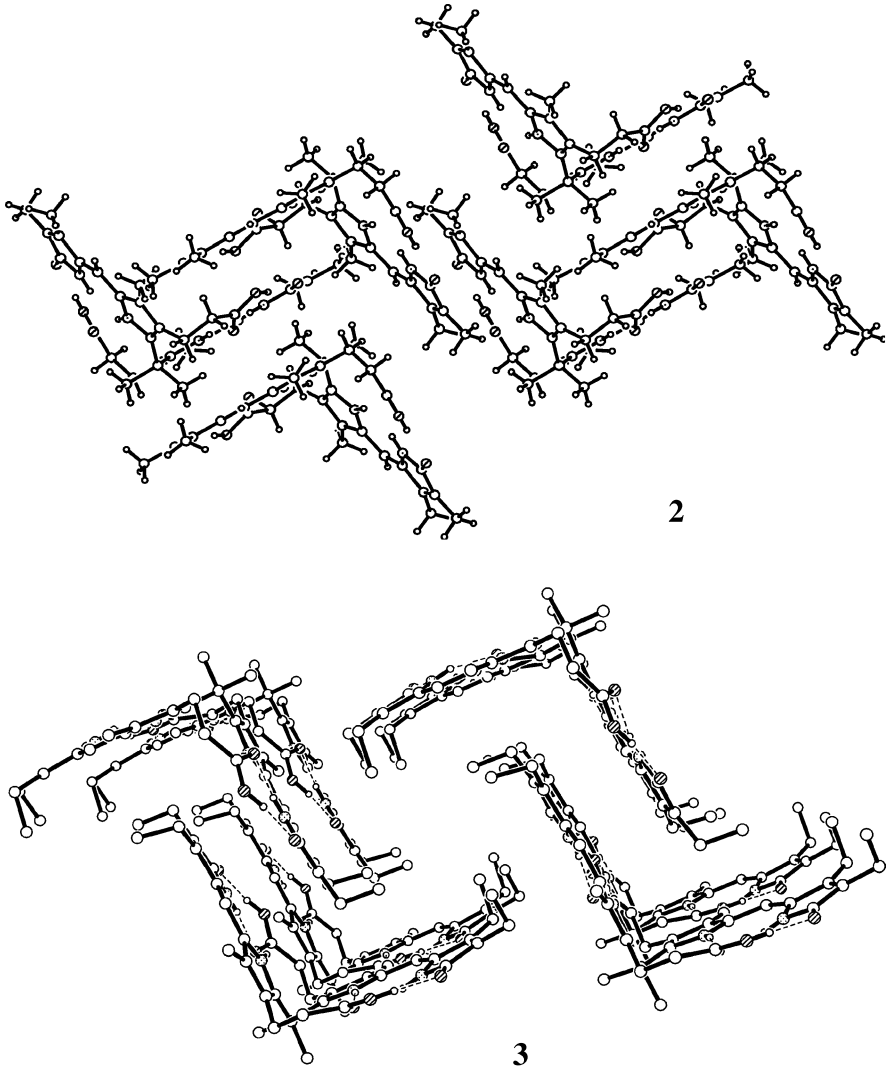

Fig. 4. Molecular packing of **2** (upper) and **3** (lower) in a projection showing ridge-tile conformations

Comparison of Conformation from Molecular Dynamics Calculations and X-Ray Analysis

Insight into the preferred conformations of **1**–**3** may be obtained from molecular dynamics computations as well as by crystallography. Torsion angles (ϕ_1, ϕ_2, ψ_1, ψ_2, Fig. 1A) about the carbon–carbon bonds linking the four rings are largely responsible for determining the pigment's conformation and helicity. Such torsion angles and helical pitch can be extracted from atomic coordinates of the minimum energy conformation determined by molecular dynamics calculations [3, 4] and by crystallography [3, 7, 9]. Comparison of the torsion angles obtained by both techniques for bilirubin and its *gem*-dimethyl analogs **1**–**3** are made in Table 1.

Significantly, molecular dynamics calculations, which do not take into account crystal packing forces, reproduce the experimental data for **2** and **3** reasonably

Table 2. Comparison of hydrogen bond distances, (*d*), and hydrogen bond angles, (°), from X-ray crystallography and molecular dynamics (MD);[a] calculations for lactam (L) NH, pyrrole (P) NH, and acid (OH) for 10,10-dimethylrubins **1**–**3** and bilirubin (**BR**)

Structure/Method		Hydrogen Bond Distance/Å			Hydrogen Bond Angle/°		
		LN–H···O	PN–H···O	O–H···O	LN–H···O	PN–H···O	O–H···O
1	X-ray	2.00	2.21	–	155	165	–
		1.96	2.27	–	158	141	–
	MD	1.48	1.57	–	172	174	–
		1.46	1.58	–	161	170	–
2	X-ray	1.98	2.12	1.77	153	168	166
		1.94	2.13	1.75	159	166	166
	MD	1.51	1.65	1.55	158	176	170
		1.52	1.65	1.55	158	176	170
3	X-ray	1.95	2.22	1.66	165	155	172
		1.97	2.11	1.71	157	171	174
	MD	1.50	1.74	1.53	163	171	172
		1.51	1.73	1.53	162	170	171
BR[b]	X-ray	1.8	1.8	1.5	160	157.3	180
					162	157	180
	MD	1.6	1.6	1.5	153	164	169
					152	165	169

[a] Using Sybyl V. 6.9 for the SGI workstation, Refs. [4a, 20]; [b] data taken from X-ray diffraction coordinates given in Ref. [5a]

well, predicting slightly smaller torsion angles (ϕ_1 and ϕ_2) about C(9)–C(10) and C(10)–C(11) and a 92–93° dihedral angle (θ) between the two planes (Table 1). The calculations predict slightly more distortion from planarity around the ψ_1/ψ_2 torsion angles in the dipyrrinone chromophores of **1**–**3**, but more planar exocyclic double bonds. The calculations reveal global minimum energy conformations of **2**, **3**, and bilirubin are very similar. Unlike computations of **2** and **3**, which are intramolecularly hydrogen bonded in the crystal, the computed energy-minimum conformation of **1** cannot reasonably be expected to reproduce the conformation of **1** in the crystal where X-ray crystallography shows the pigment molecules to be linked by intermolecular hydrogen bonds. Molecular dynamics calculations of **1** find a ridge-tile shape as the lowest energy conformation, even without the benefit of stabilization from intramolecular hydrogen bonds. In the crystal, however, stabilization from intermolecular dipyrrinone to dipyrrinone hydrogen bonds and crystal packing forces give a different conformation (Fig. 2), one that is an extended shape with dipyrrinone NHs *syn* to the $C(CH_3)_2$ group.

A comparison of hydrogen bond distances and hydrogen bond angles in **2**, **3**, and bilirubin from their crystal structures and their global minimum energy structures determined by molecular dynamics calculations is given in Table 2. The hydrogen bond distances are distinctly longer in crystals of **2** and **3** than in the

computed energy-minimized structure, with lesser differences observed in bilirubin: the computed N–H···O=C hydrogen bonds are some 25% shorter, and the O–H···O=C hydrogen bonds ~20% shorter – all relative to molecules in the crystal. Whether the differences are due to crystal packing forces or to parameterization in the Sybyl forcefield [26] is unclear. All computed and "observed" (X-ray) hydrogen bond angles of **2** and **3** lie within ~20° of optimum angle of 180°. The O–H···O and lactam N–H···O angles are nearly identical in the computed and observed but the computed pyrrole N–H···O angles differ from one another by 10–15°. The differences may be related to the molecular dynamics computations predicting planar exocyclic C=C bonds.

Crystal Packing

The stacking pattern in **2** and **3** is very similar to that found in bilirubin and mesobilirubin (Figs. 3 and 4) [5]. The ridge-tiles are stacked with their dipyrrinone systems parallel to one another (at the *van der Waals* distance) (Figs. 3 and 4), thereby giving rise to channels in the crystal lattice in which disordered solvent molecules reside. Stacks of ridge-tile shaped molecules of **2** and **3** interleave with similar but inverted stacks. There is little evidence for *intermolecular* association as the hydrogen bond pattern is almost exclusively *intramolecular*. The stacking pattern described here is very characteristic of intramolecularly hydrogen-bonded ridge-tile conformers of bilirubins [9, 10] but it is very different than the stacking pattern of those bilirubins which cannot or do not attain ridge-tile conformations in the solid state [9, 25]. This is in clear contrast to the molecular packing of the dimethyl ester (Fig. 2), where molecules of **1** adopt an extended conformation and are linked by intermolecular hydrogen bonds into supramolecular ribbons.

Experimental

gem-Dimethyl-rubins **1**–**3** were prepared as reported previously [17]. Crystals were grown by slow diffusion of *n*-hexane into a solution of CH_2Cl_2 or $CHCl_3$. A crystal was placed onto the tip of a 0.1 mm diameter glass capillary and mounted on a Bruker SMART Apex system for data collection at 100(2) K. A preliminary set of cell constants was calculated from reflections harvested from 3 sets of 20 frames. These initial sets of frames were oriented such that orthogonal wedges of reciprocal space were surveyed. Final orientation matrices were determined from least squares refinement of 3653 reflections for **1**, 1924 for **2**, and 6380 for **3** harvested from the final data collection. The data collection was carried out using MoKα radiation (0.71073 Å graphite monochromator) with a frame time of 10 seconds and a detector distance of 4.9 cm. A randomly oriented region of reciprocal space was surveyed to the extent of 2 hemispheres and to a resolution of 0.68 Å. Four major sections of frames were collected with 0.3° steps in ω at 600 different ϕ settings and a detector of 35° in 2θ. The intensity data were corrected for absorption and decay (SADABS) [27]. Final cell constants were calculated from the xyz centroids of strong reflections from the actual data collection after integration (SAINT 6.01, 1999) [28]. Crystal data and refinement information may be found in Table 3.

The structure was solved using SHELX-93 [28] and refined using SHELX-97 [29]. The space groups *P*-1 and *P*-2(1)/*c* were determined based on systematic absences and intensity statistics. A direct-methods solution was calculated which provided most non-hydrogen atoms from the E-map. Full-matrix least squares/difference *Fourier* cycles were performed which located the remaining non-hydrogen atoms. All non-hydrogen atoms (Tables 4–6) were refined with anisotropic displacement parameters.

Table 3. Crystal data and structure refinement for 10,10-dimethyl rubins **1–3**

	1	**2**	**3**
Formula weight	616.75	673.62	764.16
Crystallized from	$CHCl_3$/*n*-hexane	CH_2Cl_2/*n*-hexane	$CHCl_3$/*n*-hexane
Temperature	100(2) K	100(2) K	100(2) K
Formula	$C_{35}H_{44}N_4O_6$	$C_{33}H_{40}N_4O_6 \cdot CH_2Cl_2$	$C_{37}H_{48}N_4O_6 \cdot CHCl_3$
Crystal size [mm]	$0.15 \times 0.12 \times 0.09\,mm^3$	$0.09 \times 0.07 \times 0.05\,mm^3$	$0.31 \times 0.22 \times 0.07\,mm^3$
Crystal system	Monoclinic	Triclinic	Triclinic
Space group	*P*-2(1)/*c*	*P*-1	*P*-1
Z	4	2	2
Unit cell dimensions	$a = 10.7874(6)$ Å	$a = 8.4689(6)$ Å	$a = 11.9353(19)$ Å
	$b = 21.6840(11)$ Å	$b = 11.8331(8)$ Å	$b = 12.533(2)$ Å
	$c = 16.4799(8)$ Å	$c = 17.3383(11)$ Å	$c = 14.722(3)$ Å
	$\alpha = 90°$	$\alpha = 74.720(2)°$	$\alpha = 73.497(9)°$
	$\beta = 106.2300(10)°$	$\beta = 83.3240(10)°$	$\beta = 69.332(8)°$
	$\gamma = 90°$	$\gamma = 73.4210(10)°$	$\gamma = 84.718(9)°$
Volume	3701.3(3) $Å^3$	1604.84(49) $Å^3$	1975.5(6) $Å^3$
Density (calculated)	$1.259\,Mg/m^3$	$1.394\,Mg/m^3$	$1.285\,Mg/m^3$
Absorption coefficient	$0.224\,mm^{-1}$	$0.255\,mm^{-1}$	$0.281\,mm^{-1}$
F(000)	1488	712	808
Crystal habit and color	block, yellow	block, yellow	rhomboid, yellow
Theta range for data collection	1.88 to 27.50°	1.22 to 28.8°	1.54 to 30.51°
Index ranges	$-13 \le h \le 14$	$-11 \le h \le 11$	$-17 \le h \le 16$
	$-28 \le k \le 24$	$-15 \le k \le 15$	$-17 \le k \le 17$
	$-19 \le l \le 21$	$-23 \le l \le 23$	$-20 \le l \le 21$
Reflections collected	26852	19065	26833
Independent reflections	8459	7917	11864
	[*R*(int) = 0.0576]	[*R*(int) = 0.0683]	[*R*(int) = 0.0312]
Observed reflections ($I > 2\sigma(I)$)	5629	4578	7997
Completeness to theta	27.50°, 99.5%	28.28°, 99.4%	30.51°, 98.6%
Absorption correction	SADABS	SADABS	SADABS
Max. and min. transmission	0.9797 and 0.9668	0.9884 and 0.9767	0.9811 and 0.9182
Refinement method	Full-matrix least-squares on F^2	Full-matrix least-squares on F^2	Full-matrix least-squares on F^2
Data/restraints/parameters	8459/0/443	7917/0/423	11864/18/683
Goodness-of-fit on F^2	1.092	0.985	1.094
Final *R* indices	$R1 = 0.0724$	$R1 = 0.0587$	$R1 = 0.0572$
[$I > 2\sigma(I)$]	$wR2 = 0.2060$	$wR2 = 0.1192$	$wR2 = 0.1557$
R indices (all data)	$R1 = 0.1099$	$R1 = 0.1187$	$R1 = 0.0884$
	$wR2 = 0.2254$	$wR2 = 0.1399$	$wR2 = 0.1782$
Largest diff. peak and hole	0.596 and $-1.023\,e.Å^{-3}$	0.848 and $-0.655\,e.Å^{-3}$	0.516 and $-0.516\,e.Å^{-3}$

Table 4. Atomic coordinates ($\times 10^4$) and equivalent isotropic displacement parameters ($Å^2 \times 10^3$) for **1**; U(eq) is defined as one third of the trace of the orthogonalized U^{ij} tensor

	x	y	z	U(eq)
O(1)	21(2)	3970(1)	2218(1)	21(1)
C(1)	544(3)	4171(1)	1688(2)	17(1)
C(1S)	688(5)	9076(2)	−232(3)	49(1)
Cl(1S)	−549(1)	8529(1)	−573(1)	60(1)
Cl(2S)	722(1)	9375(1)	760(1)	54(1)
C(2)	958(3)	3824(1)	1047(2)	17(1)
C(3)	1423(3)	4233(1)	582(2)	15(1)
C(4)	1332(2)	4854(1)	912(2)	13(1)
C(5)	1675(3)	5379(1)	586(2)	14(1)
C(6)	1713(3)	6014(1)	821(2)	14(1)
C(7)	2238(3)	6485(1)	448(2)	14(1)
C(8)	2155(3)	7038(1)	884(2)	14(1)
C(9)	1572(3)	6897(1)	1507(2)	15(1)
C(10)	1232(3)	7321(1)	2155(2)	15(1)
C(11)	2402(3)	7720(1)	2551(2)	14(1)
C(12)	3660(3)	7546(1)	2921(2)	14(1)
C(13)	4410(3)	8089(1)	3146(2)	15(1)
C(14)	3567(3)	8591(1)	2910(2)	14(1)
C(15)	3920(3)	9229(1)	3015(2)	15(1)
C(16)	3222(3)	9752(1)	2921(2)	14(1)
C(17)	3760(3)	10379(1)	3027(2)	15(1)
C(18)	2768(3)	10786(1)	2892(2)	16(1)
O(19)	446(2)	10632(1)	2613(1)	19(1)
C(19)	1564(3)	10434(1)	2725(2)	16(1)
N(21)	804(2)	4779(1)	1590(2)	16(1)
N(22)	1306(2)	6278(1)	1469(1)	13(1)
N(23)	2349(2)	8351(1)	2556(1)	14(1)
N(24)	1886(2)	9826(1)	2725(2)	16(1)
C(21)	802(3)	3138(1)	964(2)	21(1)
C(31)	1917(3)	4106(1)	−162(2)	21(1)
C(71)	2811(3)	6414(1)	−276(2)	19(1)
O(81)	3978(2)	8792(1)	741(2)	33(1)
C(81)	2649(3)	7655(1)	701(2)	17(1)
C(82)	4123(3)	7695(1)	986(2)	20(1)
O(82)	5875(2)	8372(1)	1431(2)	39(1)
C(83)	4624(3)	8349(1)	1031(2)	25(1)
C(84)	6464(4)	8980(2)	1524(3)	57(1)
C(101)	46(3)	7707(1)	1689(2)	20(1)
C(102)	904(3)	6953(1)	2865(2)	21(1)
C(121)	4188(3)	6900(1)	3049(2)	17(1)
O(121)	4047(3)	5581(1)	3770(2)	49(1)
C(122)	4430(3)	6666(1)	3965(2)	23(1)
O(122)	6058(3)	5919(1)	4323(2)	40(1)
C(123)	4800(4)	5993(1)	4009(2)	30(1)
C(124)	6516(5)	5288(2)	4370(3)	58(1)

(*continued*)

Table 4 (*continued*)

	x	*y*	*z*	*U*(eq)
C(131)	5824(3)	8112(1)	3544(2)	23(1)
C(171)	5171(3)	10510(1)	3242(2)	22(1)
C(181)	2791(3)	11477(1)	2920(2)	22(1)

Table 5. Atomic coordinates ($\times 10^4$) and equivalent isotropic displacement parameters ($Å^2 \times 10^3$) for **2**; *U*(eq) is defined as one third of the trace of the orthogonalized U^{ij} tensor

	x	*y*	*z*	*U*(eq)
O(1)	5410(2)	6068(2)	5279(1)	24(1)
C(1)	5751(3)	6979(2)	5380(2)	20(1)
C(1S)	−3091(4)	3368(3)	6317(2)	45(1)
Cl(1)	−1742(1)	3238(1)	7042(1)	61(1)
Cl(2)	−2352(1)	2218(1)	5789(1)	36(1)
C(2)	7113(3)	7495(2)	5026(2)	20(1)
C(3)	6972(3)	8482(2)	5309(1)	18(1)
C(4)	5534(3)	8628(2)	5863(1)	17(1)
C(5)	4995(3)	9443(2)	6320(1)	18(1)
C(6)	3675(3)	9582(2)	6911(1)	18(1)
C(7)	3349(3)	10381(2)	7409(2)	19(1)
C(8)	1961(3)	10203(2)	7924(1)	17(1)
C(9)	1428(3)	9317(2)	7720(1)	16(1)
C(10)	−92(3)	8820(2)	7927(2)	18(1)
C(11)	417(3)	7432(2)	8231(1)	16(1)
C(12)	112(3)	6456(2)	8026(1)	17(1)
C(13)	787(3)	5398(2)	8628(2)	18(1)
C(14)	1518(3)	5733(2)	9179(2)	17(1)
C(15)	2359(3)	4951(2)	9870(2)	19(1)
C(16)	3097(3)	5177(2)	10441(2)	18(1)
C(17)	3968(3)	4304(2)	11123(2)	19(1)
C(18)	4508(3)	4905(2)	11553(2)	19(1)
O(19)	4379(2)	7065(2)	11318(1)	25(1)
C(19)	4050(3)	6200(2)	11142(2)	20(1)
N(21)	4849(3)	7674(2)	5872(1)	21(1)
C(21)	8379(4)	6961(2)	4450(2)	28(1)
N(22)	2488(3)	8940(2)	7117(1)	17(1)
N(23)	1265(3)	6986(2)	8922(1)	17(1)
N(24)	3210(3)	6314(2)	10497(1)	19(1)
C(31)	8104(3)	9301(2)	5101(2)	24(1)
C(71)	4281(3)	11295(2)	7383(2)	25(1)
O(81)	3863(2)	9113(2)	10277(1)	26(1)
C(81)	1307(3)	10919(2)	8547(2)	20(1)
O(82)	1808(2)	8737(2)	9769(1)	23(1)
C(82)	2477(4)	10640(2)	9221(2)	23(1)
C(83)	2685(3)	9400(2)	9778(2)	21(1)

(*continued*)

Table 5 (*continued*)

	x	*y*	*z*	*U*(eq)
C(101)	−1096(3)	9244(2)	7167(2)	23(1)
C(102)	−1253(3)	9353(2)	8570(2)	22(1)
O(121)	2840(2)	5423(2)	6011(1)	26(1)
C(121)	−755(3)	6403(2)	7327(2)	20(1)
O(122)	1747(2)	7249(2)	6285(1)	23(1)
C(122)	336(3)	5685(2)	6760(2)	22(1)
C(123)	1709(3)	6204(2)	6334(2)	20(1)
C(131)	767(3)	4115(2)	8669(2)	23(1)
C(171)	4196(3)	2953(2)	11285(2)	25(1)
C(181)	5416(3)	4443(2)	12306(2)	26(1)

Table 6. Atomic coordinates ($\times 10^4$) and equivalent isotropic displacement parameters ($Å^2 \times 10^3$) for **3**; *U*(eq) is defined as one third of the trace of the orthogonalized U^{ij} tensor

	x	*y*	*z*	*U*(eq)
O(1)	−2282(1)	−1461(1)	4684(1)	33(1)
C(1)	−1290(2)	−1453(1)	4795(1)	26(1)
C(1S)	4694(2)	2775(2)	4542(2)	62(1)
Cl(1)	4813(3)	3063(2)	5605(2)	69(1)
Cl(3)	5631(2)	1706(2)	4252(3)	65(1)
Cl(2)	5106(2)	4079(2)	3599(2)	76(1)
Cl(1A)	4712(6)	3236(6)	5486(5)	192(3)
Cl(2A)	5089(3)	3584(3)	3345(2)	139(2)
Cl(3A)	5604(5)	1540(5)	4451(5)	159(2)
C(2)	−957(2)	−2021(1)	5678(1)	26(1)
C(3)	189(2)	−1726(1)	5475(1)	25(1)
C(4)	638(2)	−997(1)	4448(1)	23(1)
C(5)	1744(2)	−547(1)	3934(1)	23(1)
C(6)	2268(1)	119(1)	2915(1)	22(1)
C(7)	3477(1)	386(1)	2412(1)	24(1)
C(8)	3624(1)	1009(1)	1405(1)	23(1)
C(9)	2501(1)	1105(1)	1303(1)	21(1)
C(10)	2006(1)	1562(1)	439(1)	22(1)
C(11)	987(1)	2364(1)	745(1)	20(1)
C(12)	−213(1)	2472(1)	821(1)	21(1)
C(13)	−625(1)	3489(1)	1072(1)	21(1)
C(14)	322(1)	3978(1)	1156(1)	21(1)
C(15)	287(1)	5005(1)	1418(1)	23(1)
C(16)	1168(1)	5580(1)	1455(1)	22(1)
C(17)	1043(2)	6578(1)	1819(1)	25(1)
C(18)	2126(2)	6840(1)	1799(1)	26(1)
O(19)	4085(1)	5974(1)	1259(1)	29(1)
C(19)	2992(2)	6032(1)	1400(1)	24(1)
N(21)	−320(1)	−874(1)	4089(1)	25(1)

(*continued*)

Table 6 (*continued*)

	x	*y*	*z*	*U*(eq)
C(21)	−1811(2)	−2804(2)	6573(1)	36(1)
N(22)	1697(1)	565(1)	2222(1)	21(1)
C(22)	−1931(2)	−3892(2)	6350(2)	43(1)
N(23)	1289(1)	3279(1)	951(1)	21(1)
N(24)	2382(1)	5324(1)	1192(1)	24(1)
C(31)	926(2)	−2103(2)	6149(1)	31(1)
C(32)	1560(2)	−3193(2)	6053(2)	42(1)
C(71)	4449(2)	29(2)	2854(2)	35(1)
O(81)	5265(1)	4147(1)	1064(1)	33(1)
C(81)	4827(2)	1453(1)	654(1)	28(1)
O(82)	3765(1)	3541(1)	757(1)	29(1)
C(82)	5374(2)	2310(1)	939(1)	29(1)
C(83)	4718(1)	3394(1)	905(1)	25(1)
C(101)	2947(2)	2202(2)	−554(1)	29(1)
C(102)	1614(2)	558(1)	212(1)	29(1)
O(121)	−736(1)	26(1)	2296(1)	30(1)
C(121)	−1008(2)	1735(1)	652(1)	25(1)
C(122)	−2078(2)	1225(1)	1586(1)	26(1)
O(122)	−2684(1)	−36(1)	3198(1)	40(1)
C(123)	−1762(2)	347(1)	2392(1)	25(1)
C(131)	−1842(2)	3980(1)	1193(1)	27(1)
C(171)	−125(2)	7140(2)	2190(2)	36(1)
C(172)	−803(3)	6627(2)	3301(2)	61(1)
C(181)	2488(2)	7698(2)	2174(2)	35(1)
C(182)	2887(3)	7160(2)	3072(2)	54(1)

The data were corrected for absorption using an empirical model. Hydrogen atom positions were placed in ideal positions and refined as riding atoms with relative isotropic displacement parameters (a C–H distance fixed 0.96 Å and a thermal parameter 1.2 times the host carbon atom). Tables of bond lengths and angles, anisotropic displacement parameters, hydrogen coordinates, and isotropic displacement parameters have been deposited at the Cambridge Structural Data, file [CCDC No. 227591 for **1**, CCDC No. 227592 for **2**, CCDC No. 227593 for **3**].

Acknowledgments

We thank the U.S. National Institutes of Health (HD-17779) for generous support of this work, and the National Science Foundation (CHE-0226402) for providing the funds to purchase the X-ray diffractometer.

References

[1] McDonagh AF (1979) Bile Pigments: Bilatrienes and 5,15-Biladienes. In: Dolphin D (ed) The Porphyrins, vol 6. Academic Press, New York, p 293

[2] Chowdhury JR, Wolkoff AW, Chowdhury NR, Arias IM (2001) Hereditary Jaundice and Disorders of Bilirubin Metabolism. In: Scriver CR, Beaudet AL, Sly WS, Valle D (eds) The Metabolic & Molecular Basis of Inherited Disease, vol II. McGraw-Hill, Inc, New York, pp 3063–3101

[3] Falk H (1989) The Chemistry of Linear Oligopyrroles and Bile Pigments. Springer, Wien
[4] Person RV, Peterson BR, Lightner DA (1994) J Am Chem Soc **116**: 42
[5] a) Bonnett R, Davies JE, Hursthouse MB, Sheldrick GM (1978) Proc R Soc London, Ser B **202**: 249; b) LeBas G, Allegret A, Mauguen Y, DeRango C, Bailly M (1980) Acta Crystallogr, Sect B **B36**: 3007; c) Becker W, Sheldrick WS (1978) Acta Crystallogr, Sect B **B34**: 1298
[6] Nogales DF, Ma JS, Lightner DA (1997) Tetrahedron **49**: 2361
[7] a) Huggins MT, Lightner DA (2000) J Org Chem **65**: 6001; b) Huggins MT, Lightner DA (2000) Tetrahedron **56**: 1997; c) Boiadjiev SE, Anstine DT, Lightner DA (1994) Tetrahedron: Asymm **5**: 1945
[8] Huggins MT, Lightner DA (2001) Monatsh Chem **132**: 203
[9] For a review of crystal structures of linear polypyrrolic compounds, see Sheldrick WS (1983) Israel J Chem **23**: 155
[10] Mugnoli A, Manitto D, Monti D (1983) Acta Crystallogr, Sect C **39**: 287
[11] Brown SP, Zhu XX, Saalwächter K, Spiess HW (2001) J Am Chem Soc **123**: 4275
[12] a) Kaplan D, Navon G (1983) Israel J Chem **23**: 177; b) Kaplan D, Navon G (1983) Org Magn Res 198; c) Kaplan D, Navon G (1982) Biochem J **201**: 605; d) Navon G, Frank S, Kaplan D (1984) J Chem Soc Perkin Trans 2, 1145
[13] a) Doerner T, Knipp B, Lightner DA (1997) Tetrahedron **53**: 2697; b) Nogales D, Lightner DA (1995) J Biol Chem **270**: 73
[14] Boiadjiev SE, Person RV, Puzicha G, Knobler C, Maverick E, Trueblood KN, Lightner DA (1992) J Am Chem Soc **114**: 10123
[15] a) Falk H, Müller N (1982) Monatsh Chem **112**: 1325; b) Falk H, Müller N (1983) Tetrahedron **39**: 1875
[16] a) Shelver WL, Rosenberg H, Shelver WH (1992) Intl J Quantum Chem **44**: 141; b) Alagona G, Ghio C, Agresti A, Pratesi R (1997) Intl J Quantum Chem **70**: 395; c) Alagona G, Ghio C, Monti S (2000) Phys Chem Chem Phys **2**: 4884
[17] Kar AK, Tipton AK, Lightner DA (1999) Monatsh Chem **130**: 833
[18] Tipton A, Lightner DA (2002) Monatsh Chem **133**: 707
[19] a) Xie M, Lightner DA (1993) Tetrahedron **49**: 2185; b) Xie M, Holmes DL, Lightner DA (1993) Tetrahedron **49**: 9235
[20] Brower JO, Huggins MT, Boiadjiev SE, Lightner DA (2000) Monatsh Chem **131**: 1047
[21] Bernett MJ, Tipton AK, Huggins MT, Reeder JH, Lightner DA (2000) Monatsh Chem **131**: 239
[22] a) Cullen DL, Black PS, Meyer EF, Lightner DA, Quistad GB, Pak C-S (1977) Tetrahedron **33**: 477; b) Cullen DL, Pepe G, Meyer Jr EF, Falk H, Grubmayr K (1979) J Chem Soc Perkin Trans 2, 999
[23] Huggins MT, Lightner DA (2001) Monatsh Chem **132**: 203
[24] Kratky C, Jorde C, Falk H, Thirring K (1983) Tetrahedron **39**: 1859
[25] Sheldrick WS, Borkenstein A, Blacha-Puller M, Gossauer A (1977) Acta Crystallogr **B33**: 3625
[26] Molecular mechanics and dynamics calculations employed to find the global energy minimum conformations of **1** were run on an SGI Octane workstation using vers. 6.9 of the Sybyl forcefield as described in Refs. [4, 14, 20]; for the Ball and Stick drawings were created from the atomic coordinates using *Müller* and *Falk's* "Ball and Stick" program for the Macintosh (http://www.orc.uni-Linz.ac.at/mueller/ball_and_stick.shtml).
[27] Blessing R (1995) Acta Crystallogr **A51**: 33.
[28] SAINT 6.1, Bruker Analytical X-Ray Systems, Madison, WI, USA
[29] SHELXTL-Plus 5.10, Bruker Analytical X-Ray Systems, Madison, WI, USA